

MULTIPLICITY DISTRIBUTION IN IMPACT PARAMETER SPACE

NORISUKE SAKAI⁺)

Max-Planck-Institute for Physics and Astrophysics
Föhringer Ring 6, München 40, Germany



Abstract : We summarize the formulation of inclusive overlap functions which give multiplicity distributions at incident impact parameter b . Several models of multiperipheral type are discussed. It is pointed out that the dependence of the momentum-transfer slope upon subenergies is important in knowing which collision, central or peripheral, has higher multiplicity.

Résumé : On passe en revue la formulation de fonctions de recouvrement inclusives qui donnent des distributions de multiplicité à paramètre d'impact de la particule incidente b . Plusieurs modèles de type multi-périphérique sont discutés. On remarque que la manière dont la pente en moment transféré dépend des sous-énergies est importante pour connaître quel type de collisions, centrale ou périphérique, a une multiplicité plus élevée.

⁺) Address after September 1974 : Rutherford High Energy Laboratory, Chilton, Didcot, Berkshire, England.

1. Introduction

High energie elastic scattering can be understood as the shadow of multiparticle production by means of the s-channel unitarity relation⁽¹⁾. One of the most interesting questions in this approach is: which collision has higher multiplicity, central or peripheral? A new formalism, called inclusive overlap function, has been recently presented⁽²⁾ in order to analyze the multiplicity distribution as a function of incident impact parameter b .

The purpose of this report is to summarize the previous results on the inclusive overlap function and to add the analysis of several models. Inclusive overlap functions are defined and the generalized unitarity relation is stated in the next section. Consequences of the assumption of the dominance of a simple factorizable Pomeron pole are described in Sect. 3. Inclusive overlap functions in a multiperipheral model (MPM) with the Chew-Pignotti approximation and in the absorbed MPM are calculated in Sect. 4. The final section is devoted to a discussion of the average squared impact parameter as a function of multiplicity. We point out the importance of an experimental determination of the dependence of the slope in momentum transfer upon subenergies in the final state.

2. Generalized unitarity and inclusive overlap functions

The well-known optical theorem is the unitarity relation in the s-channel at $t = 0$ ($t = (p'_a - p_a)^2 = (p_b - p'_b)^2$)
(1) $\sigma_{\text{tot}} = \text{Im } f_{\text{el}} (t=0)$
The s-channel unitarity relation at general t is
(2) $0(t) = \text{Im } f_{\text{el}} (t)$

where $0(t)$ is the overlap function,⁽³⁾ whose Fourier transform gives the cross section $\sigma(b)$ at incident impact parameter b . Mueller first noted the generalized optical theorem which gives the single-particle inclusive cross section in terms of an appropriate absorptive part of three-body forward elastic amplitude⁽⁴⁾⁽⁵⁾

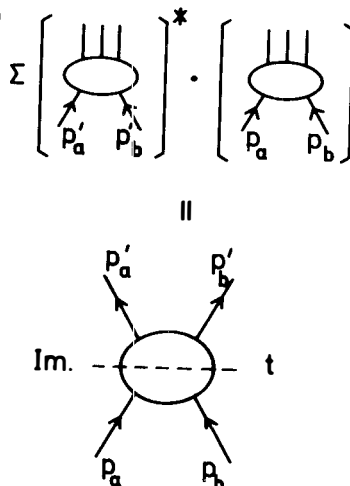


Fig. 1

$$(3) \quad \omega \frac{d\sigma}{d^3 q} = \text{Abs. } f_6(t=0)$$

In a recent publication⁽²⁾, we have generalized the Mueller's optical theorem to a full unitarity relation in the missing-mass channel at general $t = (p_a' - p_a)^2$

$$(4) \quad \omega \frac{d\sigma}{d^3 q} = \text{Abs. } f_6(t)$$

The left-hand side is defined by an overlap integral for two multiparticle S-matrix elements and is called the single-particle inclusive overlap function. For details, see ref. 2.

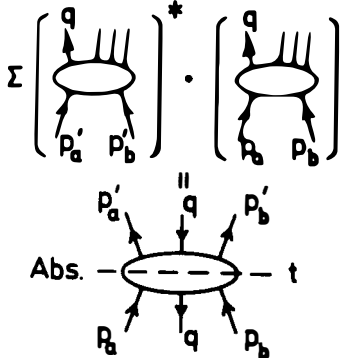


Fig. 2

If we decompose final states into various multiplicities, we obtain $\sigma_{\text{tot}} = \sum_n \sigma_n$,

$$(5) \quad \sigma(t) = \sum_n \sigma_n(t),$$

$$\text{and } \int \frac{d^3 q}{\omega} \omega \frac{d\sigma}{d^3 q} = \sum_n n \sigma_n,$$

$$(6) \quad \Sigma_1(t) \equiv \int \frac{d^3 q}{\omega} \omega \frac{d\sigma}{d^3 q} = \sum_n n \sigma_n(t)$$

The Fourier transform in terms of the momentum transfer $p_a' - p_a$ gives the impact parameter representation in the incident channel

$$(7) \quad \begin{aligned} \sigma(t) &\rightarrow \sigma(b) = \sum_n \sigma_n(b), \\ \Sigma_1(t) &\rightarrow \tilde{\Sigma}_1(b) = \sum_n n \sigma_n(b) \end{aligned}$$

Therefore the average multiplicity as a function of the incident impact parameter is given by

$$(8) \quad \bar{n}(b) = \sum_n n \sigma_n(b) / \sum_n \sigma_n(b) = \tilde{\Sigma}_1(b) / \sigma(b)$$

which can be obtained from the two- and three-body elastic scattering amplitude.

The above consideration can be extended to many-particle inclusive overlap functions and the set of all such inclusive overlap functions is equivalent to the information on the complete multiplicity distributions in impact parameter space.

3. Simple factorizable Pomeron pole

Pomeron exchange in elastic scattering gives the overlap function in Fig. 3

$$(9) \quad \Omega(t) = e^{(\alpha_p(t) - 1)Y} \beta_a(t) \beta_b(t)$$

where β is the Pomeron-two-particle vertex, $\alpha_p(t)$ the Pomeron trajectory, $Y = \log(s/m^2)$ the total rapidity.

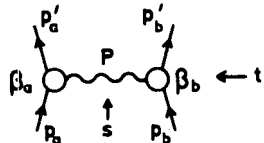


Fig. 3

The dominant contribution to the inclusive overlap function at high energies comes from the pionization region and is given in terms of two-Pomeron-two-particle coupling $\bar{c}(\vec{q}_\perp, t)$

$$(10) \quad \Omega \frac{d\Sigma_1(t)}{d^3 q} = \Omega(t) \cdot \bar{c}(\vec{q}_\perp, t)$$

$$\omega_1 \omega_2 \frac{d\Sigma_2(t)}{d^3 q_1 d^3 q_2} = \Omega(t) \cdot \bar{c}(\vec{q}_1^\perp, t) \cdot \bar{c}(\vec{q}_2^\perp, t)$$

and so on. Therefore the average multiplicity $\bar{n}(b)$ and the correlation parameter $f_2(b)$ as functions of impact parameter are given by

$$(11) \quad \bar{n}(b) = \tilde{c} * \sigma(b) Y / \sigma(b)$$

$$f_2(b) = \tilde{c} * \tilde{c} * \sigma(b) Y^2 / \sigma(b) - (\bar{n}(b))^2$$

where \tilde{c} means the Fourier transform of $c(t) = \int d^2 q_\perp \bar{c}(\vec{q}_\perp, t)$ and $*$ means the convolution integral $\tilde{c} * \sigma = (2\pi)^{-1} \int d^2 b' c(b') \sigma(b - b')$. Using the experimental fact that the overlap function is approximately exponential in t , we obtain in Fig. 6 a representative curve for $\bar{n}(b)$ and $f_2(b)$ in the case of a smooth space-like decreasing function $c(t)$.

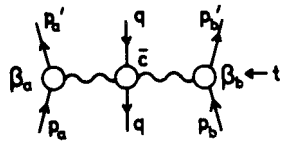


Fig. 4

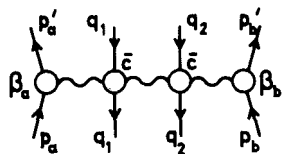


Fig. 5

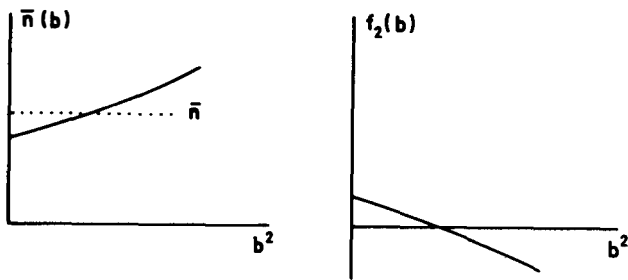


Fig. 6

4. Multiperipheral-type models (MPM) for exclusive processes

4.1 Simplified model in the Chew-Pignotti approximation

The matrix element is given by⁽⁶⁾

$$M = \frac{25}{m^4} e^{\alpha_0 Y} \prod_{i=0}^n M_i(z_i, \vec{q}_i) \quad (12)$$

$$M_i(z_i, \vec{q}_i) \propto \theta(z_i) \sqrt{a_i} e^{-a_i \vec{q}_i^2}$$

$$a_i = \bar{a}_i + \alpha' z_i$$

$$\bar{a}_i = \bar{a} \quad \text{for } i = 1, \dots, n-1$$

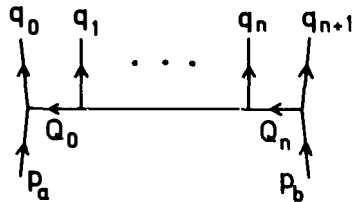


Fig. 7

where z_i is the rapidity difference and Q_i the transverse momentum transfer of the i -th step, and α_0 and α' are the intercept and the slope of the Regge trajectory exchanged in the multiperipheral chain.

Using high energy approximation

$$(13) \quad x_i \approx 0 \quad \text{for } i = 1, \dots, n-1$$

$$x_0 \approx 1 \quad x_{n+1} \approx -1$$

where

$$x_i = \frac{2q_i/\sqrt{s}}{\sqrt{s}}$$

we obtain

$$(14) \quad \begin{aligned} 0(t) &= d(t) \exp \left[\{c(t) + 2\alpha_0 - 2 + \frac{\alpha' t}{2} \} \right] \\ &\omega \frac{d\Sigma_1(t)}{d^3 q} = 0(t) \cdot \bar{c}(\vec{q}_1, t) \end{aligned}$$

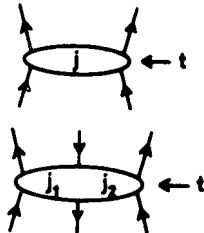
$$\omega_1 \omega_2 \frac{d\Sigma_2(t)}{d^3 q_1 d^3 q_2} = 0(t) \cdot \bar{c}(\vec{q}_1, t) \cdot \bar{c}(\vec{q}_2, t)$$

and so on, where

$$(15) \quad \begin{aligned} \bar{c}(\vec{q}, t) &= c(t) \cdot \frac{\bar{a}}{\pi} \exp(-\bar{a} \vec{q}, t)^2, \\ c(t) &= c_0 e^{\alpha' t} \end{aligned}$$

Leading singularity in j -plane corresponds to a simple factorizable pole at $j = \sigma_p(t)$

$$(16) \quad \sigma_p(t) = 2\alpha_0 - 1 + \frac{\alpha'}{2} t + c(t).$$



4.2 Absorbed MPM

For comparison, we calculate inclusive overlap functions of the self-consistent MPM with absorption (7)(8). Multiplicity distributions in impact parameter space have been worked out in ref. 8. Using it, we obtain the leading singularity of the t -channel partial wave amplitudes for the absorptive part of the two- and three-body elastic amplitudes.

Fig. 8

$$(17) \quad \begin{aligned} I_m f_{ee}(j; t) &\propto \frac{1}{\{(j-1)^2 - R^2 t\}^{\frac{3}{2}}} \\ \text{Abs. } f_6(j_1, j_2, t) &\propto \frac{1}{j_1 - j_2} \left[\frac{1}{(j_2-1)\{(j_2-1)^2 - R^2 t\}} - \frac{1}{(j_1-1)\{(j_1-1)^2 - R^2 t\}} \right] \end{aligned}$$

The leading singularity is at $j = 1 \pm iR/\sqrt{-t}$ and non-factorizable, which corresponds to a fully absorbing sphere of radius RY . The average multiplicity is given by⁽⁸⁾

$$(18) \quad \bar{n} (b) \propto \sqrt{Y^2 - \left(\frac{b}{R}\right)^2}$$

5. Average squared impact parameter $\bar{b}^2(n)$

Let us now examine a complementary quantity, the average squared impact parameter $\bar{b}^2(n)$ as a function of multiplicity. We take a matrix element for the configuration in Fig. 9

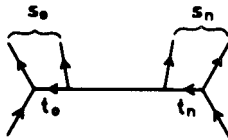


Fig. 9

$$(19) \quad M = F \cdot \exp \left(\sum_{i=0}^n a_i t_i \right)$$

where F and a_i are functions of s_i and s , and we neglect the t_i -dependent phase. An exact expression for $\bar{b}^2(n)$ in this case was derived⁽⁹⁾ which gives, in a high energy approximation (13),

$$(20) \quad \bar{b}^2(n) = 2 \left\langle \sum_{i=0}^n a_i \right\rangle$$

where $\langle \rangle$ means the averaging.

The Chew-Pignotti model in the Sect. 4.1 gives $a_i = a + 'z_i$, so we find

$$(21) \quad \bar{b}^2(n) \cong 2 \left(\bar{a} n + \sigma' Y \right)$$

i.e. higher multiplicities are more peripheral.

In the CLA model⁽¹⁰⁾, a_i is given by

$$(22) \quad a_i = \log_e \left(1 + \frac{s'}{b_i} \right)$$

where b_i are parameters and

$$(23) \quad s'_i = s_i - (m_i + m_{i+1})^2 \simeq 2m_{iT}m_{i+1T} \cosh(y_i - y_{i+1})$$

For small multiplicities $s_i' \simeq \frac{\overline{m_T^2}}{b} e^{y_i - y_{i+1}}$
and we obtain a decreasing function of
 $n(\log(\frac{\overline{m_T^2}}{b}) < 0)$

$$(24) \quad \overline{b^2}(n) \simeq 2 \left\{ (n+1) \log \left(\frac{\overline{m_T^2}}{b} \right) + Y \right\}$$

We can estimate the behavior⁽¹¹⁾ of $\overline{b^2}(n)$
for large n , by assuming equal spacing in
rapidity

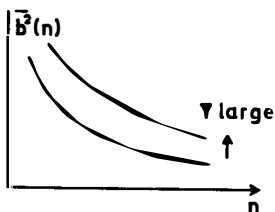


Fig. 10

$$(25) \quad \overline{b^2}(n) \simeq 2(n+1) \log \left(1 + \frac{\overline{m_T^2}}{b} 2 \cosh \frac{Y}{n+1} \right)$$

which is illustrated in Fig. 10.

In the absorbed MPM in Sect. 4.2., large shrinkage in each multi-peripheral step ($a_i \propto (y_i - y_{i+1})^2$) forces $\overline{b^2}(n)$ small as n increases, although the formula (20) is not directly applicable because of the absorption factor.

As a conclusion, we would like to stress the importance of obtaining experimental information of the dependence of the momentum-transfer slope upon subenergies, in order to see which collision, central or peripheral, has higher multiplicity.

References

1. For a recent review, see H.I. Miettinen: the Proceeding of the Second Aix-en-Provence International Conference on Elementary Particles, Suppl. Jour. Phys., 34, C1-263 (1973).
2. N. Sakai: Multiplicity Distribution in Impact Parameter Space and Inclusive Overlap Functions, MPI preprint, to be published in Nuovo Cimento.
3. L. Van Hove: Nuovo Cimento 28, 798 (1963); Rev. Mod. Phys. 36, 665, (1964).
4. A.H. Mueller: Phys. Rev. D2, 2963 (1970).
5. H.P. Stapp: Phys. Rev. D3, 3177 (1971); C.I. Tan, Phys. Rev. D4, 2412 (1971).
6. G.F. Chew and A. Pignotti: Phys. Rev. 176, 2112 (1968).
7. J. Finkelstein and F. Zachariasen: Phys. Lett. 34B, 631 (1971).
8. L. Caneshi and A. Schwimmer: Nucl. Phys. B44, 31 (1972).
9. J. Turnau: Acta Phys. Polon. 36, 7 (1969).
10. H.M. Chan, J. Loskiewicz, and W.W.M. Allison: Nuovo Cimento 57A, 93, (1968).
11. Realistic Monte Carlo calculations have recently been performed, showing this feature of decreasing $b^2(n)$, S. Jadach and J. Turnau, Overlap Function from the Multiperipheral Model, Cracow preprint (1974); see also L. Michejda, J. Turnau, and A. Bialas, Nuovo Cimento, A56, 241 (1968). We thank Dr. A. Bialas for bringing these references into our attention.